APL Materials

Antimony doped tin oxide/ polyethylenimine electron selective contact for reliable and light soaking-free high performance inverted organic solar cells

Cite as: APL Mater. **7**, 091103 (2019); https://doi.org/10.1063/1.5115260
Submitted: 16 June 2019 . Accepted: 15 August 2019 . Published Online: 05 September 2019

Efthymios Georgiou, Ioannis T. Papadas, Ioanna Antoniou, Marek F. Oszajca, Benjamin Hartmeier, Michael Rossier, Norman A. Luechinger, and Stelios A. Choulis

AIP Publishing

Antimony doped tin oxide/polyethylenimine electron selective contact for reliable and light soaking-free high performance inverted organic solar cells

Cite as: APL Mater. 7, 091103 (2019); doi: 10.1063/1.5115260
Submitted: 16 June 2019 • Accepted: 15 August 2019 •
Published Online: 5 September 2019

Efthymios Georgiou,[1] Ioannis T. Papadas,[1] Ioanna Antoniou,[1] Marek F. Oszajca,[2] Benjamin Hartmeier,[2] Michael Rossier,[2] Norman A. Luechinger,[2] and Stelios A. Choulis[1,a)]

AFFILIATIONS

[1]Molecular Electronics and Photonics Research Unit, Department of Mechanical Engineering and Materials Science and Engineering, Cyprus University of Technology, 45 Kitiou Kyprianou Street, Limassol, 3603, Cyprus
[2]Avantama Ltd., Stafa, Laubisrutistr. 50, Zurich CH-8712, Switzerland

[a)]E-mail: stelios.choulis@cut.ac.cy

ABSTRACT

We have demonstrated a high-performance low temperature solution processed electron selective contact consisting of 10 at. % antimony doped tin oxide (ATO) and the neutral polymer polyethylenimine (PEI). Inverted organic photovoltaics (OPVs) utilizing ATO/PEI as electron selective contact exhibited high power conversion efficiencies for both the reference P3HT:PCBM and the nonfullerene based P3HT:IDTBR active layer OPV material systems. Importantly, it is shown that the proposed ATO/PEI carrier selective contact provides light soaking-free inverted OPVs. Furthermore, by increasing the thickness of the ATO layer from 40 to 120 nm, the power conversion efficiency of the corresponding inverted OPVs remain unaffected, a parameter which indicates the potential of the proposed ATO/PEI carrier selective contact for high performance light-soaking-free and reliable roll-to-roll printing solutions processed inverted OPVs.

The ability to fabricate ultrathin, lightweight, flexible, and low-cost photovoltaics trigger the research community and industries in a depth investigation of organic photovoltaics (OPVs) during the last two decades. The power conversion efficiency (PCE) and the lifetime performance of OPVs are continuously improving. Recent progress in OPVs overcame the barrier of 10% certified power conversion efficiency.[1] In addition, the progress of the lifetime performance of OPVs during the previous years resulted in OPVs with promising long term stability.[2] Development of high performance solution processed electronic materials is one of the key OPV product development targets since the application of roll to roll printing manufacturing determine the potential of OPVs for future low-cost next generation photovoltaics.

The development of inverted OPVs provided an interesting architecture,[3] since it allowed studying fundamental processes in organic bulk heterojunction architecture, including the vertical phase segregation of polymer/fullerene blends as well as the charge selectivity of the metal-oxide based carrier selective contacts.[3,4] Metal oxides have been extensively used as n-type or p-type buffer layers in inverted OPVs due to their high transparency, relatively high conductivity, tunable work function, and solution processability. Furthermore, the advantage of solution processing of these materials at low temperatures provides opportunities for low cost, reliable, and roll-to-roll process up-scalable OPVs. Solution processed doped metal oxides with high transparency and conductivities could meet the requirements for reliable and up-scalable roll-to-roll inverted OPVs since thicker buffer layers (100–200 nm) can be deposited without affecting significantly the device performance.[5,6] SnO_2 is an n-type, wide bandgap semiconductor that, when doped, can exhibit good transparency throughout the visible

range of the solar spectrum and low electrical resistivity. Doped tin oxides are commonly used as buffer layers for a wide range of applications including solar cells.[7,8]

The first reported metal oxide interface modification for improving the performance of inverted OPVs included the incorporation of a polyoxyethylene tridecyl ether (PTE) interfacial layer between indium doped tin oxide (ITO) and solution-processed titanium oxide.[4] Recently, Poly[(9,9-bis(3′-(N,N-dimethylamino) propyl)-2,7-fluorene)-alt-2,7-(9,9-dioctyl)-fluorene] (PFN) or Polyethylenimine (PEI) interface modification of metal-oxide based materials using several methods such as dipping, bilayer, or as additive in the precursor have also been reported in the literature to improve OPVs device performance.[9–13] In more detail, it has been shown that incorporation of PEI improves the morphology and structural order of ZnO and thereby the electron mobility in the vertical direction. Most importantly, PEI interface modification is widely used to reduce the energy levels of metal oxides and consequently the work function of bottom electrodes of inverted OPVs and thereby assist in suitable band alignment of the metal oxide with the OPV based active layer.[14] The work function modification is caused by the formation of an interfacial dipole at the interface which induces a vacuum level shifting and thereby a work function reduction.[15–17] As a result, such interface modification enhances the device performance of OPVs mainly due to improved fill factor (FF) and open circuit voltage (Voc) values.

In this work, we present a highly conductive and transparent 10 at. % antimony doped tin oxide (ATO) modified with an ultrathin PEI interfacial layer as a high performance, reliable, and light soaking-free electron selective contact (ESC) for inverted OPVs. Since the PEI interfacial layer is in the range of 5 nm, the PEI processing step can be also considered as the interface conditioning step of ATO. By applying the proposed ATO/PEI electron selective contact inverted OPV, PCEs of 3.8% were achieved with the reference poly(3-hexylthiophene) : phenyl-C61-butyric acid methyl ester (P3HT:PCBM) active layer system. The current density characteristics of the corresponding devices remain unaffected from UV light soaking, which is an important parameter for newly developed metal-oxide based carrier selective contacts. Furthermore, increasing the thickness of ATO from 40 nm to 120 nm, the power conversion efficiency of the corresponding ATO/PEI electron selective contact based inverted OPVs remain unaffected, a parameter which indicates the potential of ATO/PEI carrier selective contact for reliable roll-to-roll printing processed OPVs. Importantly, the proposed ATO/PEI electron selective contact was also applied to inverted OPVs incorporating rhodanine-benzothiadiazole-coupled indacenodithiophene (IDTBR) nonfullerene acceptor. The corresponding nonfullerene based inverted OPVs using ATO/PEI electron selective contact obtain PCE of 5.74% revealing the suitability of ATO/PEI electron selective contact for highly efficient nonfullerene acceptor based inverted OPVs.

The antimony doped tin oxide (10 at. % Sb:SnO_2) solution in mixture of butanols was developed by Avantama Ltd. The ATO powders were synthesized by Avantama Ltd. with flame spray pyrolysis. For flame spray pyrolysis, a metal organic precursor was prepared by dissolving a tin salt and an antimony salt in alkyl carboxylic acid and toluene. The metal organic precursor was fed (9 ml/min) to a spray nozzle, dispersed by oxygen (14 l/min) and ignited by a premixed methane–oxygen flame (CH_4: 1.2 l/min, O_2: 2.2 l/min). The off-gas was filtered through a metal filter (BOPP Ag) by a vacuum pump (Busch, Mink MM 1142 BV) at about 20 m^3/h. The obtained nanopowder was collected from the metal filter. The as-prepared ATO nanoparticles were stabilized in a mixture of butanol at 2.5 wt. % using an undisclosed Avantama Ltd. surfactant.

Figure 1(a) shows the X-ray diffraction pattern for the tin oxide with 10 at. % doped antimony. All the diffraction pattern shows

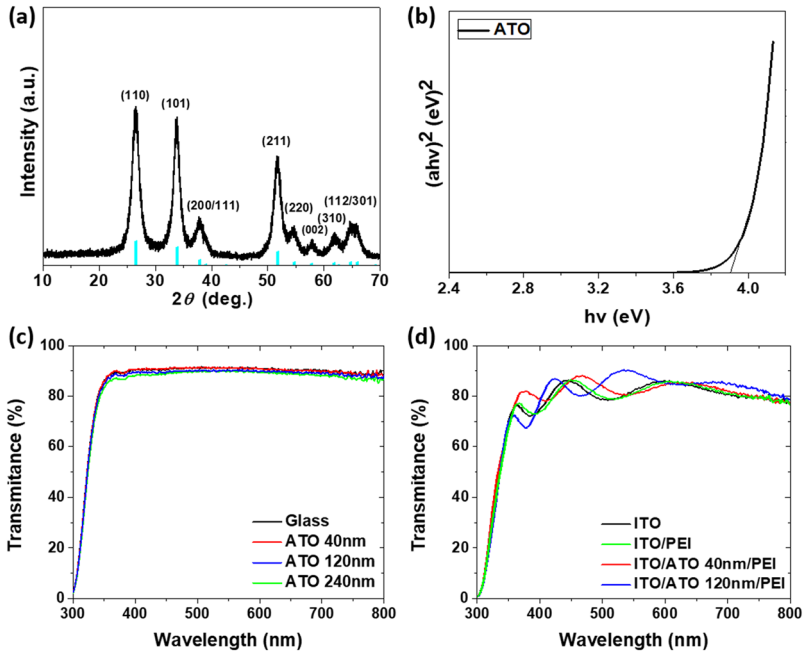

FIG. 1. (a) XRD pattern of ATO nanoparticles. The standard pattern of SnO_2 (PDF #41-1445) is also given for comparison (cyan line). (b) Tauc's plot, $(\alpha E)^2$ vs photon energy (E), showing an energy bandgap 3.9 eV of ATO NPs film fabricated on a quartz substrate. (c) Transmittance of ATO at different layer thicknesses. (d) Transmittance of the bottom electrode: ITO, ITO/PEI, ITO/ATO 40 nm/PEI, and ITO 120 nm PEI.

characteristic tin oxide peaks with the tetragonal structure (Cassiterite, Space group: $P4_2/mnm$, unit cell: $a = 4.738$ Å and $c = 3.187$ Å, PDF #41-1445). The average domain size of SnO_2 crystallites calculated from Scherrer analysis of the (110) peak width is ~5 nm. It seems that Sb dopant does not form a second phase either in or with the SnO_2. Figure 1(b), shows the corresponding Tauc plot obtained by the optical absorption spectrum of the ATO films fabricated on a quartz substrate for direct allowed transition $[(\alpha E)^2$ vs photon energy (E)]. The ATO films exhibit an intense optical absorption onset in the UV region, which is associated with an optical bandgap of 3.9 eV [Fig. 1(b)]. The observed wide optical bandgap implies a high optical transparency of the proposed ATO buffer layers in the desired wavelength range. Figure 1(c) shows the transparency of ATO buffer layers at different thickness. As shown in Fig. 1(c), ATO buffer layers present high transparency in the visible spectrum and one can observe a slight reduction of transmittance while the thickness of the ATO layer increases to 240 nm. The excellent transparency of the proposed inverted OPV bottom electrode, ITO/ATO/PEI, is shown in Fig. 1(d), which also includes the transmittance measurements of ITO and ITO/PEI bottom electrodes. In addition, the conductivity of the ATO based buffer layers was measured with the four-point probe technique resulting in values in the order of 10^{-3} S cm^{-1}, which is a targeted conductivity value of doped oxides for OPVs application.

To investigate the surface topography of ITO and ATO before and after the deposition of the ultrathin PEI interfacial layer, atomic force microscopy (AFM) images were obtained and illustrated in Fig. 2. As can be seen from Fig. 2, pristine ITO presents root mean square roughness (Rq) in the range of 4 nm and is reduced at 2.94 nm after the deposition of PEI. In general, ATO layers present smooth surface topography and relatively low Rq. The 40 nm ATO and 120 nm ATO layers present relatively the same Rq before and after PEI interface modification, from 5.9 nm to 6 and from 4.4 nm to 4.5 nm, respectively.

Figures 3(a) and 3(b) shows the illuminated and dark current density vs voltage (JV) characteristics of inverted P3HT:PCBM based OPVs with different carrier selective contact (CSC) using the

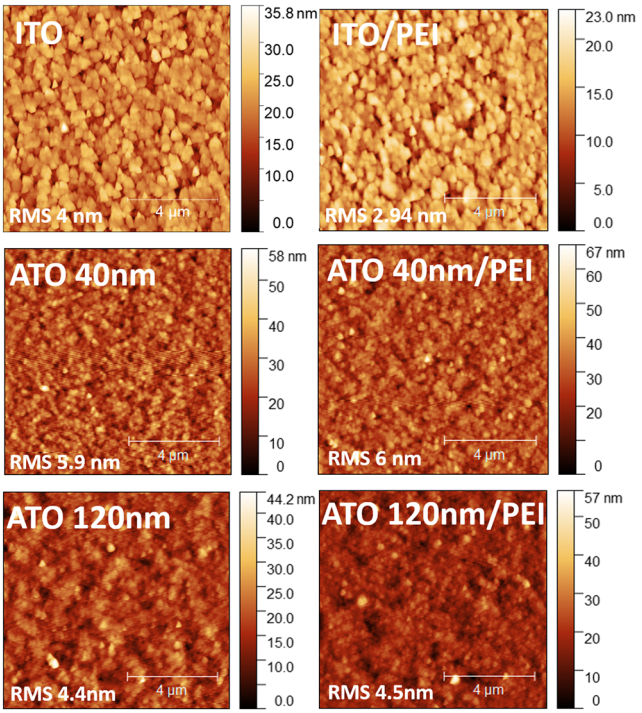

FIG. 2. AFM images of ITO, ITO/PEI, ATO 40 nm, ATO 40 nm/PEI, ATO 120 nm, and ATO 120 nm/PEI.

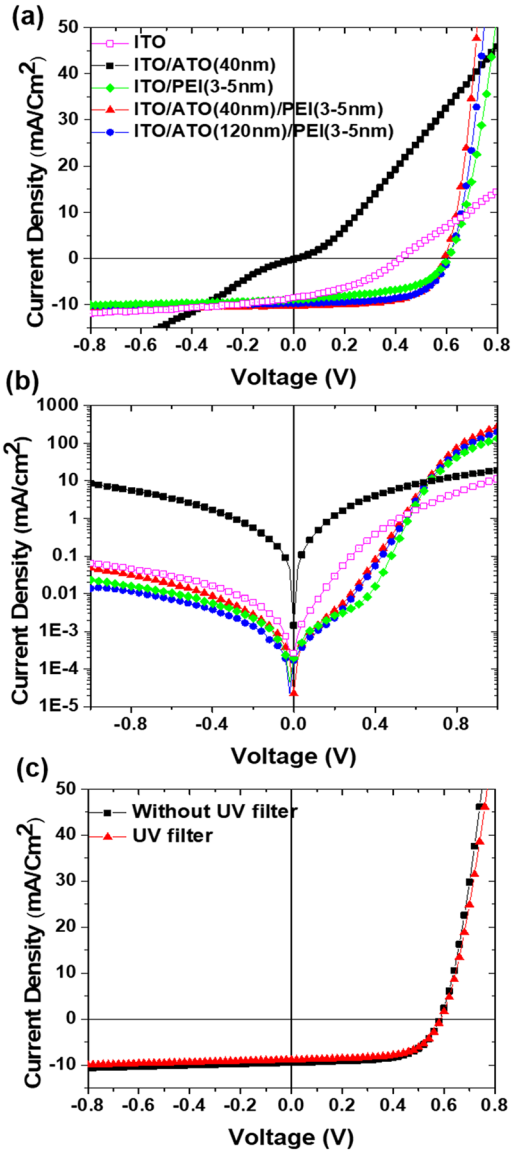

FIG. 3. (a) Illuminated JV characteristics of inverted OPVs with ATO (black squares), ATO (40 nm)/PEI (red rectangles), ATO (120 nm)/PEI (blue circles), PEI (green diamonds), and ITO only (magenta squares). (b) Dark JV characteristics. (c) JV characteristics of inverted OPVs with ATO (40 nm)/PEI as electron selective contact under AM1.5 illumination without and with UV the blocking filter ($\lambda > 400$ nm).

TABLE I. JV device performance parameters of inverted P3HT:PCBM OPVs with electron selective contact (ESC): ATO (40 nm), ATO (40 nm)/PEI, ATO (120 nm)/PEI, PEI, and without ETL (ITO only).

OPVs with ESC:	V_{oc} (V)	J_{sc} (mA cm^{-2})	FF (%)	PCE (%)
ITO	0.42	8.5	39	1.4
ITO/PEI	0.60	8.6	56	2.9
ITO/ATO 40 nm and 120 nm	NF	NF	NF	NF
ITO/ATO 40 nm/PEI	0.60	10.3	61	3.8
ITO/ATO 120 nm/PEI	0.62	9.8	61	3.7

following device configuration: ITO/CSC/P3HT:PCBM/MoO_3/Ag. As shown in Figs. 3(a) and 3(b), OPVs using just ITO have shown high leakage current and high series resistance, Rs, showing poor selectivity and thus low PCE of 1.4%. On the other hand, OPVs with ITO/PEI (modification of ITO with PEI) have shown an improvement in carrier selectivity which is reflected to better FF value and thus better device performance with a PCE of 2.9% as depicted in Table I which summarize the corresponding OPV device performance parameters. The devices using only ATO (40 or 120 nm) as the buffer layer function as a resistor (Fig. 3) show that an energetic barrier is created at the bottom electrode. According to the literature, the LUMO level of PC[60]BM is −4.7 eV, and the experimental results presented indicate an energetic barrier for electron collection at the bottom electrode due to a nonfavorable energy level alignment with ATO work function.[18] For the above reason, the device performance parameters for inverted OPVs using the ITO/ATO bottom electrode within Table I are indicated as nonfunctional (NF). Importantly, by the using the PEI interface modification, inverted OPVs using ITO/ATO/PEI as the bottom electrode were performed efficiently. The proposed ATO/PEI carrier selective contact significantly improved electron carrier selectivity in inverted OPVs. Inverted P3HT:PCBM based OPVs with 0.6 V open circuit voltage (Voc), 10.3 mA/cm^2 short circuit current (Jsc) and 61% FF and 3.8% PCE were achieved by using ITO/ATO/PEI bottom electrode as illustrated in Fig. 3. As previously reported in the literature, PEI based interface modification cause reduction of the metal-oxide work function.[9] The high photovoltaics performance of P3HT:PCBM based inverted OPV reported in this paper by using ITO/ATO/PEI bottom electrodes indicates suitable energy levels matching between the ATO/PEI and PC[60]BM that resulted to efficient electron carrier selectivity for the inverted OPVs under investigation.

Furthermore, due to high conductivity and transparency of ATO by increasing the thickness of 10 at. % doped ATO at 120 nm, the performance of P3HT:PCBM based inverted OPVs using the ITO/120 nm ATO/PEI bottom electrode remains unaffected (3.7% PCE). These results indicating that the PEI interface modification does not affect the conductivity of the 10 at. % doped ATO in the vertical direction and therefore the proposed thick ATO/PEI electron selective contact can provide a reliable buffer layer for the roll-to-roll printing processing of solution processed photovoltaics.

An obstacle of inverted OPVs using metal oxides as electron transporting layer (ETL) is the light soaking effect, in which some metal-oxide buffer layers were reported to need UV light in order to be activated.[4] In the absence of UV light (light-soaking), OPVs that use metal oxides such as TiOx or ZnO in some cases were reported to present S-shape JV characteristics and poor electron selectivity resulting in the low FF factor and PCE values.[4] Solar spectrum includes UV radiation, and it is well known that UV light is a factor that negatively affects OPVs stability. To improve OPV lifetime, encapsulation (packaging) of OPVs usually incorporate UV filter. Taking into consideration that an organic solar

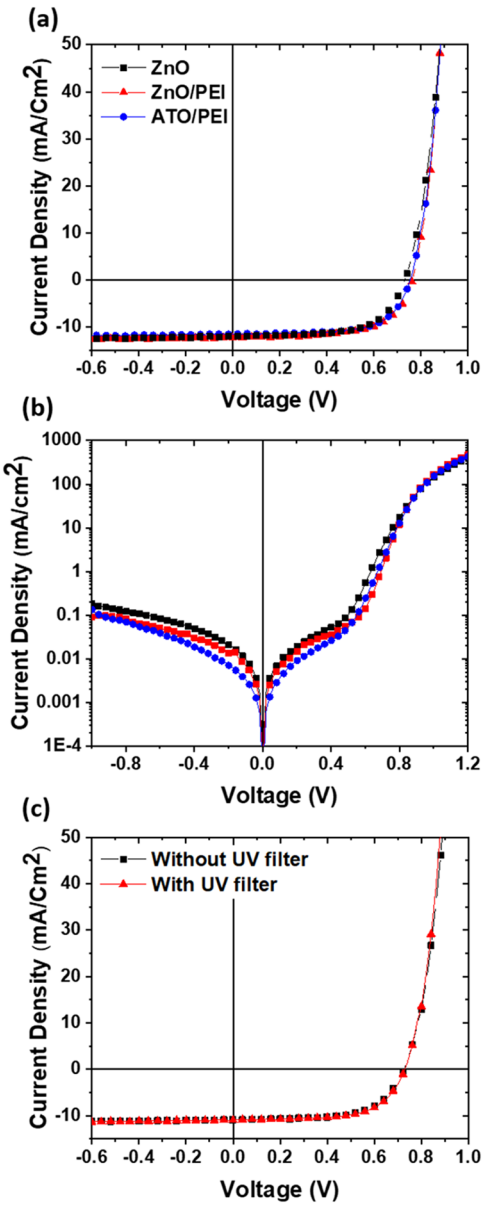

FIG. 4. (a) Illuminated JV characteristics of inverted OPVs with P3HT:IDTBR as an active layer and ETL: ZnO (black squares), ZnO/PEI (red rectangles), and ATO/PEI (blue circles), (b) Dark JV characteristics, and (c) JV characteristics of inverted OPVs with ATO (40 nm)/PEI as the electron selective contact under AM1.5 illumination without and with the UV blocking filter (λ > 400 nm).

TABLE II. JV device performance parameters of inverted OPVs with P3HT:IDTBR as the active layer and ESC: ZnO, ZnO/PEI, ATO/PEI.

OPVs with ETL:	V_{oc} (V)	J_{sc} (mA cm^{-2})	FF (%)	PCE (%)
ITO/ZnO	0.74	12.02	62.9	5.61
ITO/ZnO/PEI	0.76	12.22	63.6	5.93
ITO/ATO/PEI	0.76	11.46	65.7	5.74

cell product will need the presence of a UV-filter as part of the packaging to prevent photo-oxidization of the organic based active layer, light-soaking free carrier selective contacts are essential for the product development of inverted OPVs. It has been shown that in some cases, this phenomenon can be mitigated with the use of doped metal-oxides.[5] In addition, SnOx was reported as light soaking free ETL.[19,20] Figure 3(c) shows the illuminated JV characteristics of inverted P3HT:PCBM based OPVs using the ATO/PEI electron selective contact with and without UV-filter. To investigate light soaking issues, illuminated JV characteristics of inverted P3HT:PCBM based OPVs with ATO/PEI were obtained with a UV filter ($\lambda > 400$ nm) showing similar performance with the illuminated JV characteristics obtained without UV filter as shown in Fig. 3(c). These results provide a strong indication that the performance of the proposed ATO/PEI electron selective contact for inverted OPVs is not affected from UV-light and thus can provide light soaking free inverted structured OPVs.

Novel nonfullerene acceptor materials such as 3,9-bis(2-methylene-(3-(1,1-dicyanomethylene)-indanone))-5,5,11,11-tetrakis(4-hexylphenyl)-dithieno[2,3-d:2′,3′-′]-s-indaceno[1,2-b:5,6-b′]dithiophene) (ITIC) and IDTBR have already been used with newly synthesized conjugated polymeric donors such as Poly([2,6′-4,8-di(5-ethylhexylthienyl)benzo[1,2-b;3,3-b]dithiophene]{3-fluoro-2[(2-ethylhexyl)carbonyl]thieno[3,4-b]thiophenediyl}) (PTB7-Th) and Poly[(2,6-(4,8-bis(5-(2-ethylhexyl)thiophen-2-yl)-benzo[1,2-b:4,5-b′]dithiophene))-alt-(5,5-(1′,3′-di-2-thienyl-5′,7′-bis(2-ethylhexyl)benzo[1′,2′-c:4′,5′-c′]dithiophene-4,8-dione)] (PBDBT) achieving efficiencies that exceed 10%.[21] This remarkable progress in terms of device efficiency demonstrates the potential of large-scale production of nonfullerene based OPVs. When mixing the well-known P3HT with the nonfullerene acceptor IDTBR (LUMO: −3.9 eV, HOMO: −5.45 eV), OPVs with 6.4% PCE can be achieved.[22,23] Therefore, to further investigate the functionality of the proposed ATO/PEI electron selective contact, inverted OPVs with the well-known polymer donor P3HT and the nonfullerene acceptor IDTBR were fabricated and their JV characteristics under dark and light are shown in Fig. 4. Table II summarizes the performance parameters of the nonfullerene (P3HT:IDTBR) based inverted OPVs using the ITO/ATO/PEI bottom electrode.

PCE of 5.74% was achieved for the proposed ATO/PEI electron selective contact, whereas the reference inverted OPVs with ZnO and ZnO/PEI shown PCE of 5.61% and 5.93%, respectively. These results importantly shown that the proposed ATO/PEI electron selective contact can be effectively applied to highly efficient nonfullerene acceptor inverted structured based OPVs. To further confirm the light soaking free inverted OPV device performance for the proposed ATO/PEI carrier selective contact, illuminated JV characteristics of nonfullerene based P3HT:IDTBR inverted OPVs with the ATO/PEI electron selective contact were obtained with the UV filter ($\lambda > 400$ nm) showing similar performance with the illuminated JV characteristics obtained without the UV filter, as shown in Fig. 4(c).

To conclude, a fundamental understanding of metal oxide interfaces and their manipulation is expected to be crucial to the continued progress of solution processed OPVs. We have demonstrated that the interface of the highly conductive and transparent solution processed 10 at. % doped ATO can be effectively modified by the neutral polymer (PEI). Inverted fullerene and nonfullerene acceptor based OPVs utilizing ATO/PEI as the electron selective contact exhibited optimized and light soaking-free PCE for both P3HT:PCBM (3.8%, PCE) and P3HT:IDTBR (5.7%, PCE) active layer material systems. The high transparency and conductivity of 10 at. % doped ATO based buffer layers allowed the solution processing of high performance inverted OPVs utilizing thick ATO/PEI carrier selective contact—an important parameter for the reliable roll-to-roll printing process of OPVs and other printed optoelectronic applications.

See supplementary material for details of the proposed electron transporting layer, processing of the materials, and OPV device fabrication. Additional information of material characterization, surface topography, XRD, and other experimental results are included.

This project received funding from the European Research Council (ERC) under the European Union's Horizon 2020 research and innovation program (Grant Agreement No. 647311).

REFERENCES

[1]S. Mori, H. Oh-oka, H. Nakao, T. Gotanda, Y. Nakano, H. Jung, A. Iida, R. Hayase, N. Shida, M. Saito, K. Todori, T. Asakura, A. Matsui, and M. Hosoya, "Organic photovoltaic module development with inverted device structure," MRS Proc. **1737**, 26–31 (2015), mrsf14-1737-u17-02.

[2]C. H. Peters, I. T. Sachs-Quintana, J. P. Kastrop, S. Beaupré, M. Leclerc, and M. D. McGehee, "High efficiency polymer solar cells with long operating lifetimes," Adv. Energy Mater. **1**, 491–494 (2011).

[3]C. Waldauf, M. Morana, P. Denk, P. Schilinsky, K. Coakley, S. A. Choulis, and C. J. Brabec, "Highly efficient inverted organic photovoltaics using solution based titanium oxide as electron selective contact," Appl. Phys. Lett. **89**, 233517 (2006).

[4]R. Steim, S. A. Choulis, P. Schilinsky, and C. J. Brabec, "Interface modification for highly efficient organic photovoltaics," Appl. Phys. Lett. **92**, 227–230 (2008).

[5]T. Stubhan, I. Litzov, N. Li, M. Salinas, M. Steidl, G. Sauer, K. Forberich, G. J. Matt, M. Halik, and C. J. Brabec, "Overcoming interface losses in organic solar cells by applying low temperature, solution processed aluminum-doped zinc oxide electron extraction layers," J. Mater. Chem. A. **1**, 6004 (2013).

[6]A. Savva and S. A. Choulis, "Cesium-doped zinc oxide as electron selective contact in inverted organic photovoltaics," Appl. Phys. Lett. **102**, 233301 (2013).

[7]X. Ren, D. Yang, Z. Yang, J. Feng, X. Zhu, J. Niu, Y. Liu, W. Zhao, and S. F. Liu, "Solution-processed Nb:SnO_2 electron transport layer for efficient planar perovskite solar cells," ACS Appl. Mater. Interfaces **9**, 2421–2429 (2017).

[8]T. Z. Oo, R. Devi Chandra, N. Yantara, R. R. Prabhakar, L. H. Wong, N. Mathews, and S. G. Mhaisalkar, "Zinc tin oxide (ZTO) electron transporting buffer layer in inverted organic solar cell," Org. Electron. **13**, 870–874 (2012).

[9]B. A. E. Courtright and S. A. Jenekhe, "Polyethylenimine interfacial layers in inverted organic photovoltaic devices: Effects of ethoxylation and molecular weight on efficiency and temporal stability," ACS Appl. Mater. Interfaces **7**, 26167–26175 (2015).

[10]X. Jia, L. Zhang, Q. Luo, H. Lu, X. Li, Z. Xie, Y. Yang, Y.-Q. Li, X. Liu, and C.-Q. Ma, "Power conversion efficiency and device stability improvement of

inverted perovskite solar cells by using a ZnO:PFN composite cathode buffer layer," ACS Appl. Mater. Interfaces **8**, 18410–18417 (2016).
[11]S. Woo, W. Hyun Kim, H. Kim, Y. Yi, H.-K. Lyu, and Y. Kim, "8.9% single-stack inverted polymer solar cells with electron-rich polymer nanolayer-modified inorganic electron-collecting buffer layers," Adv. Energy Mater. **4**, 1301692 (2014).
[12]C. Liu, Z. Li, X. Zhang, W. Guo, L. Zhang, and S. Ruan, "Annealing-free ZnO:PEI composite cathode interfacial layer for efficient organic solar cells," ACS Photonics **4**, 2952–2958 (2017).
[13]X. Min, F. Jiang, F. Qin, Z. Li, J. Tong, S. Xiong, W. Meng, and Y. Zhou, "Polyethylenimine aqueous solution: A low-cost and environmentally friendly formulation to produce low-work-function electrodes for efficient easy-to-fabricate organic solar cells," ACS Appl. Mater. Interfaces **6**, 22628–22633 (2014).
[14]H.-C. Chen, S.-W. Lin, J.-M. Jiang, Y.-W. Su, and K.-H. Wei, "Solution-processed zinc oxide/polyethylenimine nanocomposites as tunable electron transport layers for highly efficient bulk heterojunction polymer solar cells," ACS Appl. Mater. Interfaces **7**, 6273–6281 (2015).
[15]Y. Zhou, C. Fuentes-Hernandez, J. Shim, J. Meyer, A. J. Giordano, H. Li, P. Winget, T. Papadopoulos, H. Cheun, J. Kim, M. Fenoll, A. Dindar, W. Haske, E. Najafabadi, T. M. Khan, H. Sojoudi, S. Barlow, S. Graham, J.-L. Bredas, S. R. Marder, A. Kahn, and B. Kippelen, "A universal method to produce low-work function electrodes for organic electronics," Science **336**, 327–332 (2012).
[16]H. Kang, S. Hong, J. Lee, and K. Lee, "Electrostatically self-assembled nonconjugated polyelectrolytes as an ideal interfacial layer for inverted polymer solar cells," Adv. Mater. **24**, 3005–3009 (2012).
[17]P. Li, G. Wang, L. Cai, B. Ding, D. Zhou, Y. Hu, Y. Zhang, J. Xiang, K. Wan, L. Chen, K. Alameh, and Q. Song, "High-efficiency inverted polymer solar cells controlled by the thickness of polyethylenimine ethoxylated (PEIE) interfacial layers," Phys. Chem. Chem. Phys. **16**, 23792–23799 (2014).
[18]J. J. Benson-Smith, L. Goris, K. Vandewal, K. Haenen, J. V. Manca, D. Vanderzande, D. D. C. Bradley, and J. Nelson, "Formation of a ground-state charge-transfer complex in polyfluorene//[6,6]-phenyl-C61 butyric acid methyl ester (PCBM) blend films and its role in the function of polymer/PCBM solar cells," Adv. Funct. Mater. **17**, 451–457 (2007).
[19]S. Trost, A. Behrendt, T. Becker, A. Polywka, P. Görrn, and T. Riedl, "Tin oxide (SnO_x) as universal 'light-soaking' free electron extraction material for organic solar cells," Adv. Energy Mater. **5**, 1500277 (2015).
[20]S. Trost, T. Becker, A. Polywka, P. Görrn, M. F. Oszajca, N. A. Luechinger, D. Rogalla, M. Weidner, P. Reckers, T. Mayer, and T. Riedl, "Avoiding photoinduced shunts in organic solar cells by the use of tin oxide (SnO_x) as electron extraction material instead of ZnO," Adv. Energy Mater. **6**, 1600347 (2016).
[21]W. Zhao, S. Zhang, and J. Hou, "Realizing 11.3% efficiency in fullerene-free polymer solar cells by device optimization," Sci. China Chem. **59**, 1574–1582 (2016).
[22]S. Holliday, R. S. Ashraf, A. Wadsworth, D. Baran, S. A. Yousaf, C. B. Nielsen, C.-H. Tan, S. D. Dimitrov, Z. Shang, N. Gasparini, M. Alamoudi, F. Laquai, C. J. Brabec, A. Salleo, J. R. Durrant, and I. McCulloch, "High-efficiency and air-stable P3HT-based polymer solar cells with a new non-fullerene acceptor," Nat. Commun. **7**, 11585 (2016).
[23]D. Baran, R. S. Ashraf, D. A. Hanifi, M. Abdelsamie, N. Gasparini, J. A. Röhr, S. Holliday, A. Wadsworth, S. Lockett, M. Neophytou, C. J. M. Emmott, J. Nelson, C. J. Brabec, A. Amassian, A. Salleo, T. Kirchartz, J. R. Durrant, and I. McCulloch, "Reducing the efficiency–stability–cost gap of organic photovoltaics with highly efficient and stable small molecule acceptor ternary solar cells," Nat. Mater. **16**, 363–369 (2016).